Journal of the European Ceramic Society **6** (1990) 273–290

Wear Mechanisms of Ceramic Cutting Tools When Machining Ferrous and Non-ferrous Alloys

G. Brandt, A. Gerendas & M. Mikus

AB Sandvik Coromant, Stockholm, Sweden

(Received 9 March 1990; accepted 19 April 1990)

Abstract

Three ceramic cutting tool grades CC 670 (based on alumina and silicon carbide whiskers) and CC 680 (based on silicon nitride) were used for the evaluation of tool life and wear mechanisms when machining a heat-resistant alloy, Inconel 718. Tool life for both grades was determined by flank wear and depth-of-cut (DOC) notch wear except at high feed rates. Flank wear was determined by chemical interaction with the workpiece material for both cutting tool materials tested. DOC notch wear was mainly determined by seizure and pull-out of tool material fragments. Comparative tests were also performed on steel SS 2541 (similar to AISI 4340) with grade CC 670 where both flank and crater wear were found to limit tool life. The main reason for the rather good wear resistance of silicon carbide reinforced alumina in Inconel 718 in contrast to its behaviour in steel was the formation of magnesia-based protective coatings.

Die Standzeiten und die Verschleißmechanismen beim Bearbeiten der hitzebeständigen Inconel 718 Legierung wurden für drei Sorten Schneidkeramik CC 670 (ein Verbund aus Aluminiumoxid und Siliziumkarbid-Whiskern) und CC 680 (basierend und Siliziumnitrid) bestimmt. Die Standzeiten beider Sorten ausgenommen bei hohen Vorschüben, waren vom Flankenabrieb und vom Verschleiß im Kerbgrund (DOC) abhängig. Der Flankenabrieb wurde bei den beiden untersuchten Schneidwerkstoffen durch chemische Reaktion mit dem Werkstück verursacht. Der Verschleiß im Kerbgrund wurde hauptsächlich durch Festfressen und durch Ausbrüche des Schneidwerkstoffs verursacht. Ferner wurden mit der Sorte CC 670 Vergleichstests an Stahl 2541 (vergleichbar mit AISI 4340) durchgeführt, wo sowohl der Flankenabrieb als auch der Kraterabrieb die Standzeit verkürzten. Die Hauptursache für die relativ gute Verschleißbeständigkeit des SiC-verstärkten Aluminiumoxids beim Bearbeiten von Inconel 718, im Gegensatz zur Stahlbearbeitung, war die Ausbildung einer MgO-haltigen Schutzschicht.

On a étudié la durée de vie et les mécanismes d'usure mis en jeu lors de l'usinage de l'alliage à haute température Inconel 718 à l'aide des nuances CC 670 (basée sur l'alumine et les whiskers de carbure de silicium) et CC 680 (basée sur le nitrure de silicium). Les durées de vie dans le cas de l'utilisation de l'une ou l'autre des nuances ont été déterminées par essai d'usure en dépouille et par essai de profondeur d'entaille (essai DOC), en excluant l'avances élevées. L'usure en dépouille a été évaluée pour les deux matériaux testés par interaction chimique avec la pièce. L'usure d'entaille DOC a été établie principalement par fixation et arrachement de fragments du matériau de coupe. Des essais comparatifs ont également été réalisés sur l'acier SS 2541 (identique à l'AISI 4340) à l'aide de la nuance CC 670; dans ce cas la durée de vie du matériau est limitée à la fois par l'usure en dépouille et par l'usure en cratère. La formation d'une couche protectrice à base de magnésie explique que la résistance à l'usure de la nuance CC 670 soit plus élevée dans le cas de l'Inconel 718 que dans celui de l'acier.

1 Introduction

Heat-resistant alloys represent a class of material for which very large increases in productivity have been obtained during the last decade, thanks to the introduction of new ceramic cutting tool materials. Heat-resistant alloys are normally machined with WC–Co grades with cutting speeds of the order of

50 m/min. With introduction of sialon materials it was possible to increase the cutting speed by a factor of five, and the silicon carbide whisker-reinforced alumina tools which have been introduced more recently have made it possible to machine at cutting speeds up to ten times faster than with cemented carbide.

2 Experimental

2.1 Cutting tool materials

Three types of cutting tool materials were used in this investigation; CC 620, an alumina-based material with additions of zirconia; CC 670, a silicon carbide whisker-reinforced alumina; and CC 680, a silicon nitride based material. Their chemical compositions are given in Table 1.

Figure 1 shows the microstructures of CC 670 and CC 680. Figure 1(a) is a section perpendicular to the hot-pressing direction for CC 670. The hot-pressing route gives rise to an anisotropic whisker distribution with silicon carbide whiskers preferably orientated in this plane. Figure 1(b) shows the microstructure of CC 680. The micrograph is a scanning electron microscopy (SEM) picture in the back-scattered (BS) mode. After polishing and carbon-coating of a cross-section, three different phases can be identified in the micrograph due to their atomic number contrast. This is mainly due to differences in yttrium content. The dark phase which contains no yttrium is beta-sialon and can be described as a solid solution of aluminium and oxygen in beta-Si_3N_4 with the general formula $Si_{6-z}Al_zO_zN_{8-z}$ where $0<0<z>4{\cdot}2$. The light-grey phase is alpha-sialon with the formula $Y_x(Si,Al)_{12}(O,N)_{16}$ where $x<2$. The light intergranular areas are partially glassy (amorphous) and partly crystalline. The glassy phase contains yttria, alumina and some nitrogen. The microstructure of CC 620 can be found elsewhere.[1]

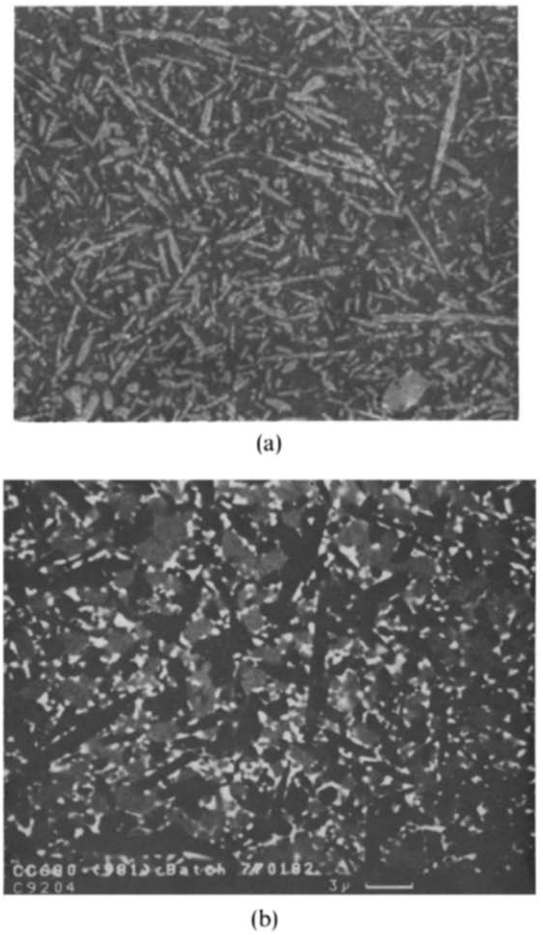

(a)

(b)

Fig. 1. Microstructures of (a) CC 670 unetched, optical, sectioned parallel to the rake face and (b) CC 680 back-scattered scanning electron micrograph.

Table 1. Chemical compositions of cutting tool materials (wt%)

	Al_2O_3	ZrO_2	Y_2O_3	SiC_w	Si_3N_4	AlN
CC 620	bal	4				
CC 670	bal			25		
CC 680	3		6		bal	10

2.2 Workpiece materials

The workpiece material was of a heat-resistant alloy Inconel 718. Comparative tests were also performed on steel SS 2541 with CC 620 and CC 670. Their chemical compositions and hardness are given in Table 2.

3 Inconel 718

3.1 Cutting conditions

The machining tests were performed as a continuous turning operation on a cylindrical bar. The original diameter and length were 180 mm and 700 mm, respectively. All cutting tests were performed wet using a 35 kW Swedturn 12 CNC lathe. The tool holder was of the block tool type with a clearance angle of 6 degrees. All inserts were in style RNGN 120700 with an edge rounding of approximately 40 microns.

Table 2. Chemical compositions (wt%) and hardness of workpiece materials

	C	Si	Mn	Cr	Mo	Ni	Fe	Al	Ti	Nb	Hardness
SS 2541	0·3	0·3	0·7	1·4	0·2	1·4	bal				HB 320
IN 718	0·04	0·3	0·2	19·0	3·0	bal	18·5	0·5	0·9	5·1	HB 370

3.2 Results

3.2.1 Tool failure modes

Figure 2 shows the tool failure modes for CC 670 and CC 680 when machining Inconel 718 at different cutting speeds and feeds. Only one cutting edge was used for each combination of cutting data in this test. The failure criteria applied to the test edges were:

(1) Flank wear greater than 0·4 mm.
(2) DOC notch wear greater than 1·0 mm.
(3) 100% rake face flaking.
(4) Total edge fracture.

As can be seen from Fig. 2 DOC notch wear is the dominating wear mechanism for CC 670 and flank wear for CC 680. Both grades exhibit fracture at the highest feed rates.

3.2.2 Tool life and wear mechanism studies

In order to study wear mechanisms and evaluate tool life a feed rate of 0·15 mm was chosen. Three edges were run for each set of cutting data in the test.

3.2.2.1 Tool life. Figure 3 shows the tool life for CC 670 and CC 680 at different cutting speeds at a feed rate of 0·15 mm/min. Tool lives are equal at 150 m/min, but significantly higher for CC 670 at higher cutting speeds.

3.2.2.2 Flank wear. Figure 4(a) shows the development of flank wear at 150 m/min. There is no difference between the two grades. Figure 4(b) shows the wear as a function of cutting time at 450 m/min. The resistance of CC 670 is much better than for CC 680.

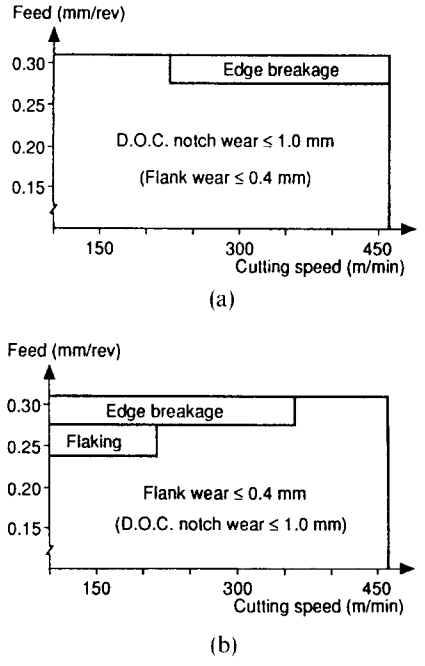

Fig. 2. Tool failure modes for (a) CC 670 and (b) CC 680 when machining Inconel 718.

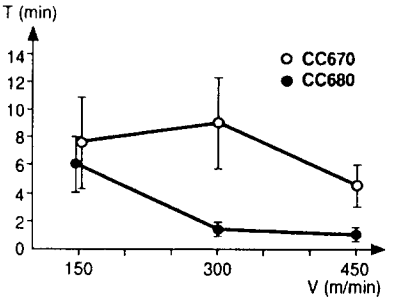

Fig. 3. Tool life versus cutting speed for CC 670 and CC 680 when machining Inconel 718 a feed rate of 0·15 mm/min and DOC 1·5 mm.

3.2.2.3 DOC notch wear. Figure 5(a) shows the DOC (depth-of-cut) notch wear at 150 m/min. As with flank wear there is no difference between the two grades. Figure 5(b) shows the notch wear at 450 m/min. CC 670 and CC 680 have the same resistance to DOC notch wear.

3.2.2.4 Notch wear at the secondary cutting edge. A feed rate of 0·25 mm/rev was chosen for this study. The wear figures for the secondary cutting edge are shown in Fig. 6(a). In contrast to the DOC notch

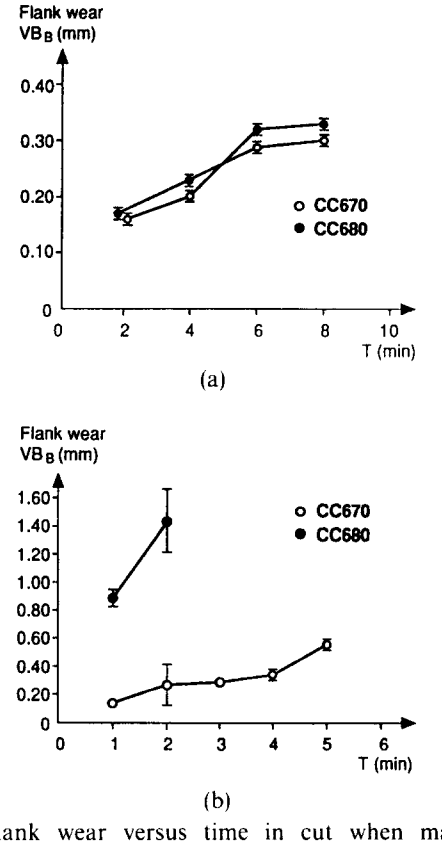

Fig. 4. Flank wear versus time in cut when machining Inconel 718 at (a) 150 m/min, 0·15 mm/rev and 1·5 mm DOC and (b) 450 m/min, 0·15 mm/rev and 1·5 DOC.

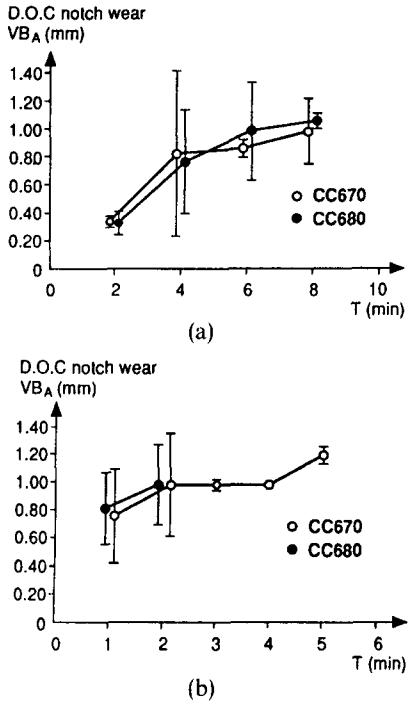

Fig. 5. DOC notch wear versus time in cut when machining Inconel 718 at (a) 150 m/min, 0·15 mm/rev and 1·5 mm DOC and (b) 450 m/min, 0·15 mm/rev and 1·5 mm DOC.

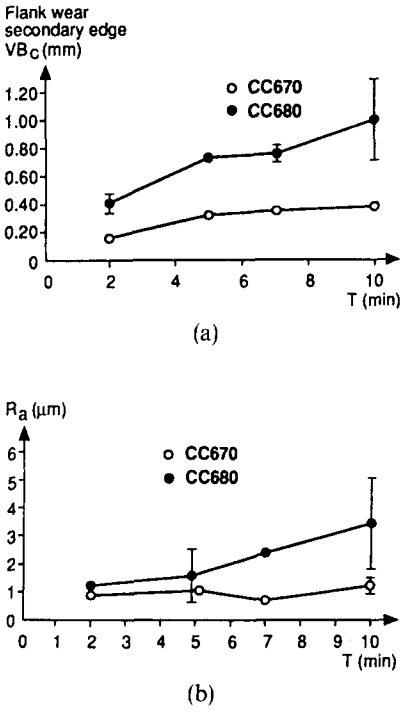

Fig. 6. (a) Flank wear on secondary cutting edge and (b) corresponding surface finish of the workpiece when machining Inconel 718 at 150 m/min, 0·25 mm/rev and 1·5 mm DOC.

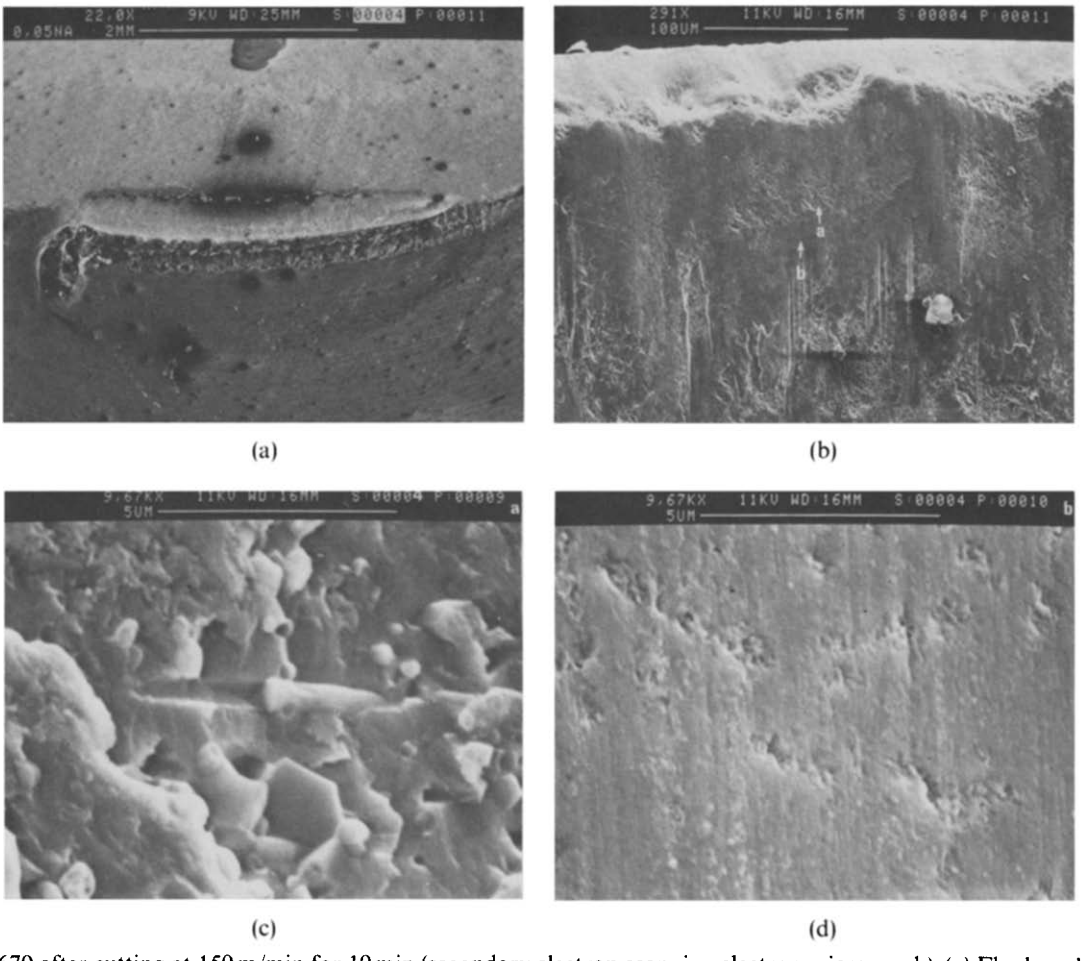

Fig. 7. CC 670 after cutting at 150 m/min for 10 min (secondary electron scanning electron micrograph). (a) Flank and DOC notch wear, (b) detail of flank wear, (c) detail of (b) marked a, detail of (b) marked b.

wear there is a large difference between the two grades. CC 670 has a much better resistance to this type of wear. The notch wear at the secondary cutting edge will directly influence the surface finish of the machined workpiece as is shown in Fig. 6(b).

3.3 Wear pattern

3.3.1 CC 670

At 150 m/min after 10 min CC 670 shows flank and DOC notch wear and small chippings along the edge line (Fig. 7(a)). The insert was first leached in a mixture of HNO_3 and HF to remove any adhering workpiece material. At higher magnification it can be seen that the flank wear consists of both rather smooth and uneven areas (Fig. 7(b)). These two different areas are shown at higher magnification in Fig. 7(c) and (d). The smooth areas are enriched with Mg which was shown using energy dispersive analysis (EDS). The uneven areas look like fracture surfaces and broken SiC whiskers can be found, Fig. 7(c). At 450 m/min the DOC notch wear is well developed (Fig. 8(a)). The flank wear (Fig. 8(b)) shows both smooth and uneven areas as for the sample at a cutting speed of 150 m/min, but in contrast the silicon carbide whiskers seem to have been partially dissolved (Fig. 8(c) and (d)) during machining.

3.3.2 CC 680

At 150 m/min after 8 min CC 680 shows flank wear and DOC notch wear (Fig. 9(a)). The upper part of the flank wear land (Fig. 9(b)) has the appearance of a fracture surface (Fig. 9(c)). This is due to small-scale fracture (chipping) along the edge line. The lower part (Fig. 9(d)) seems to be covered by a coating. EDS analysis shows the lower part of the wear land to be rich in Al. At 450 m/min after 2 min the flank wear is well developed and consists of large ridges (Fig. 10(a) and (b)). Small-scale chipping along the edge line can also be observed. The ridges are rather smooth (Fig. 10(c)), but between the ridges silicon nitride grains seem to have dissolved in the workpiece material (Fig. 10(d)).

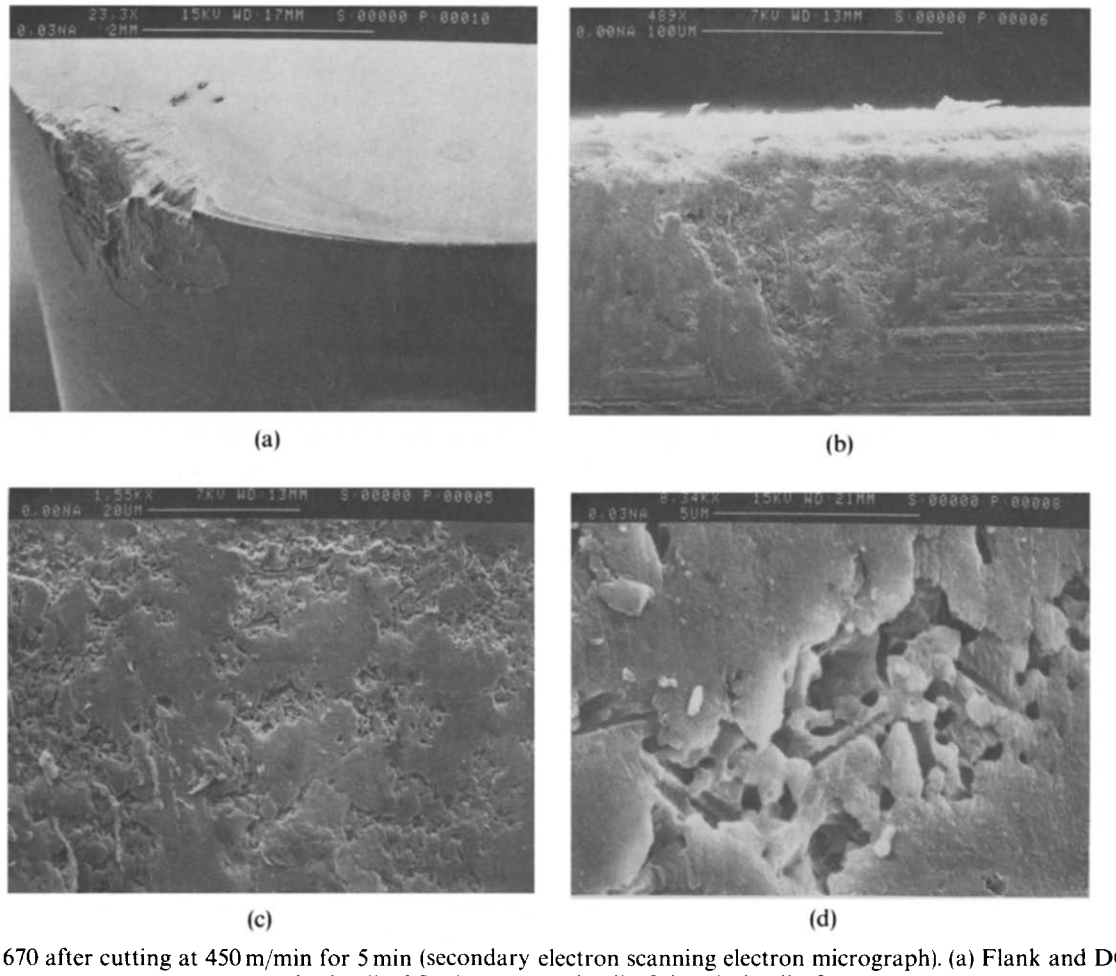

Fig. 8. CC 670 after cutting at 450 m/min for 5 min (secondary electron scanning electron micrograph). (a) Flank and DOC notch wear, (b) detail of flank wear, (c) detail of (b), (d) detail of (c).

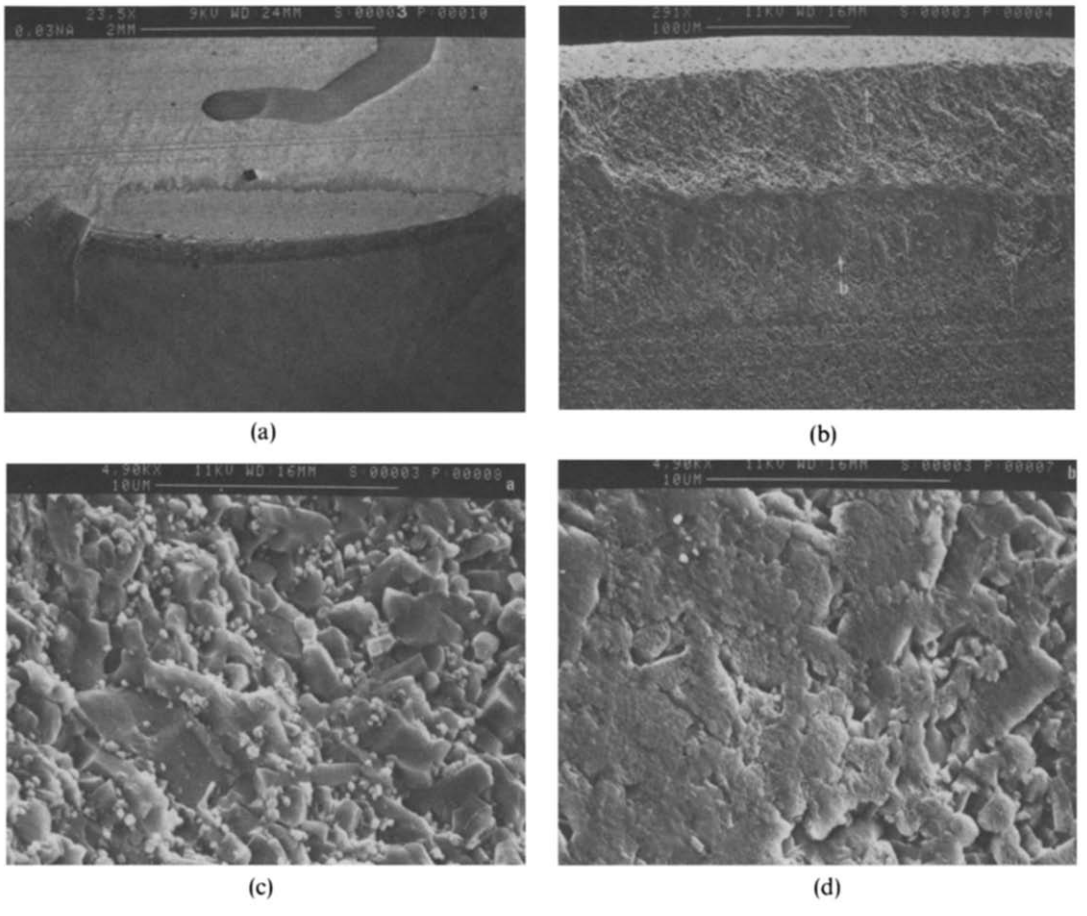

Fig. 9. CC 680 after cutting at 150 m/min for 8 min (secondary electron scanning electron micrograph). (a) Flank and DOC notch wear, (b) detail of flank wear, (c) detail of (b) marked a, detail of (b) marked b.

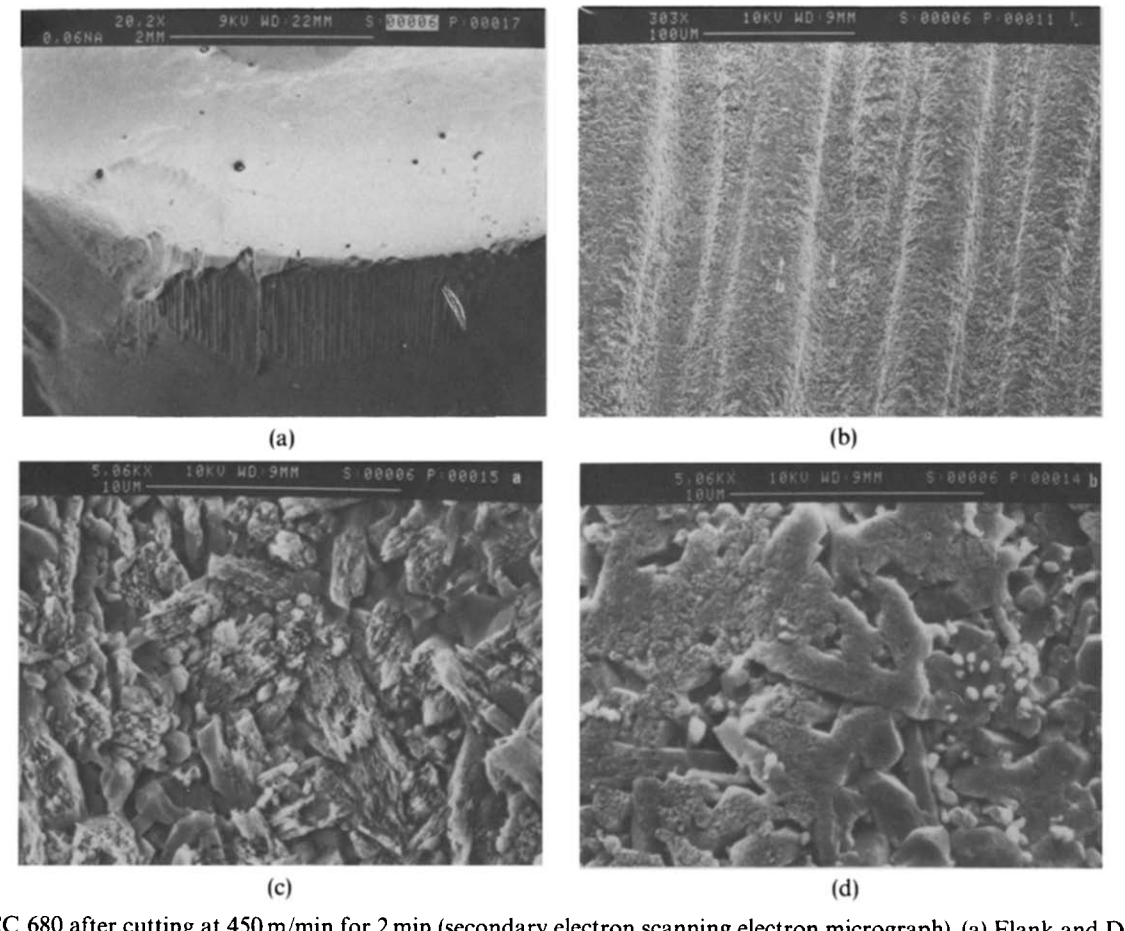

Fig. 10. CC 680 after cutting at 450 m/min for 2 min (secondary electron scanning electron micrograph). (a) Flank and DOC notch wear, (b) detail of flank wear, (c) detail of (b) marked b, (d) detail of (b) marked a.

3.4 Electron-probe microanalysis of adhering layers and tool workpiece interaction

3.4.1 CC 670

Figure 11 shows the flank face of CC 670 after machining IN 718 for 5 min at 450 m/min and 0·15 mm/rev. Layers containing mainly Mg could be observed on the lower part of the flank face.

Figure 12 shows a section perpendicular to the worn flank face. The wear is mainly concentrated on the edge line, which is typical of this type of workpiece material. Workpiece material can be observed on the lower part of the flank face. Workpiece material has also penetrated into some areas of the worn flank.

Figure 13 shows penetration of the workpiece material and its adhesion to the upper severely worn part of the flank face. It can be seen that penetration (white in the micrograph) occurs along the silicon carbide whiskers (black in the micrograph) which are probably dissolved in the metallic material. An analysis of elemental distribution from the same area shows that Fe, Cr and Ni diffuse rather a long way into the tool material whereas Ti and Nb show

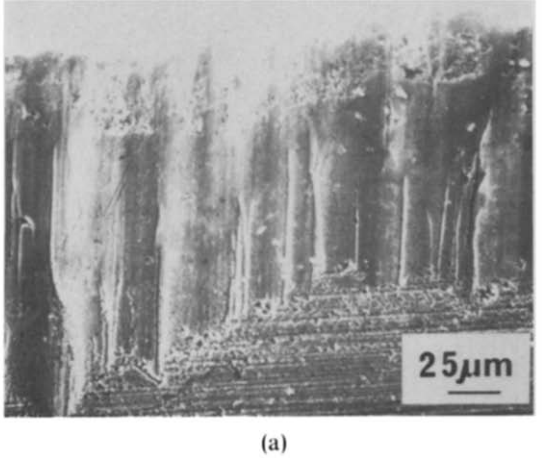

(a)

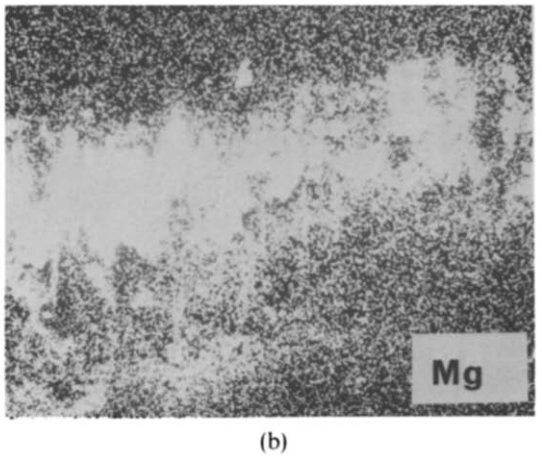

(b)

Fig. 11. Flank wear of CC 670 after machining at 450 m/min for 5 min (secondary electron scanning electron micrograph). (a) Flank wear, (b) elemental mapping of Mg.

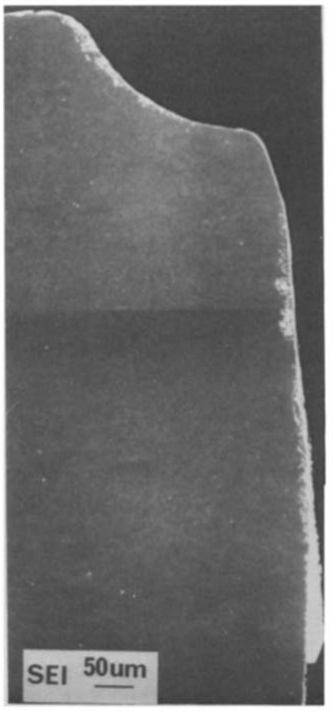

Fig. 12. Transverse section of CC 670 after machining at 450 m/min for 5 min (secondary electron scanning electron micrograph).

an enrichment at the tool surface. The silicon content decreases as the silicon carbide whiskers are dissolved but not the carbon content, which probably is a result of a reaction of carbon with the carbide-forming elements Cr, Ti and Nb in the workpiece material. The strongest carbide formers Ti and Nb react immediately with carbon and cannot therefore diffuse into the tool but Cr is less reactive and moves a further distance into the tool together with Ni and Fe.

A line scan analysis from the same area is shown in Fig. 14. From the variation of C, Ti and Cr it is obvious that TiC is formed in the surface layer whereas Cr-carbide is formed further into the tool.

Figure 15 is a section further down the flank. It shows that a thin coating of a Mg compound was formed on some areas of the worn flank. The formation of a layer of a Mg compound leads to a smaller depth of penetration of workpiece material and absence of Mg-rich layers leads to a larger penetration depth (compare Fig. 15(a) and (b)).

3.4.2 CC 680

Figure 16 shows a section through a CC 680 insert after 1·8 min at 450 m/min and 0·15 mm/min. As with CC 670 wear is concentrated to the upper part of the flank along the edge line. The cracks that are formed perpendicular to the worn face are most probably thermal in nature. CC 680 is a very thermal shock resistant material and thermal cracks

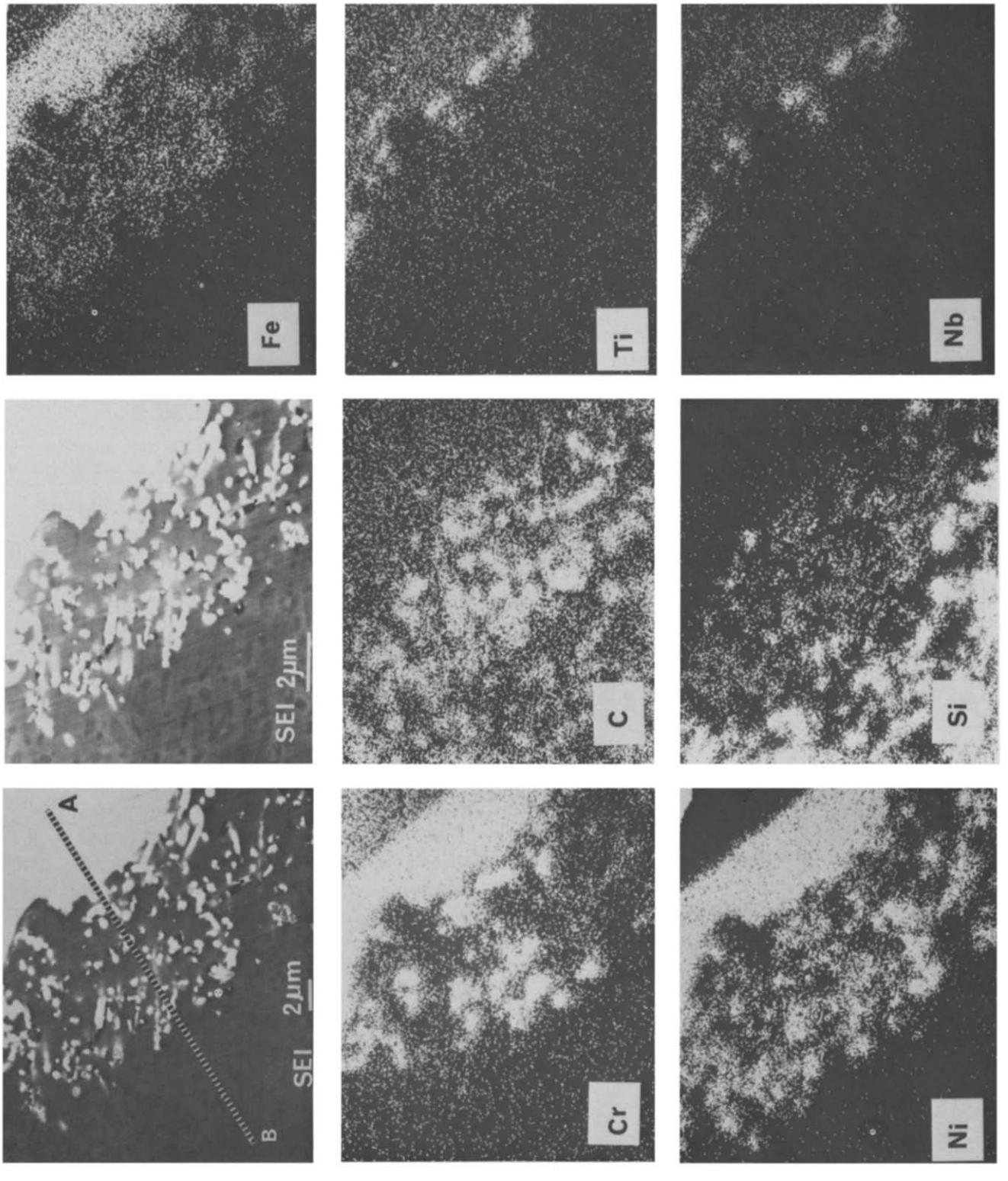

Fig. 13. Detail of Fig. 12 and corresponding element distribution.

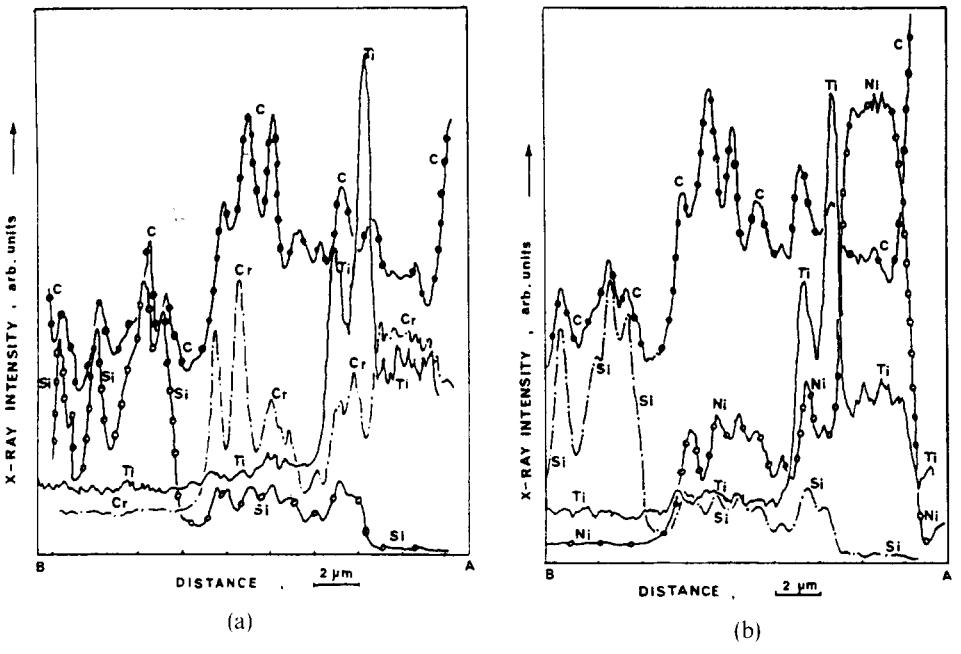

Fig. 14. Distribution of elements along the line A–B of Fig. 13.

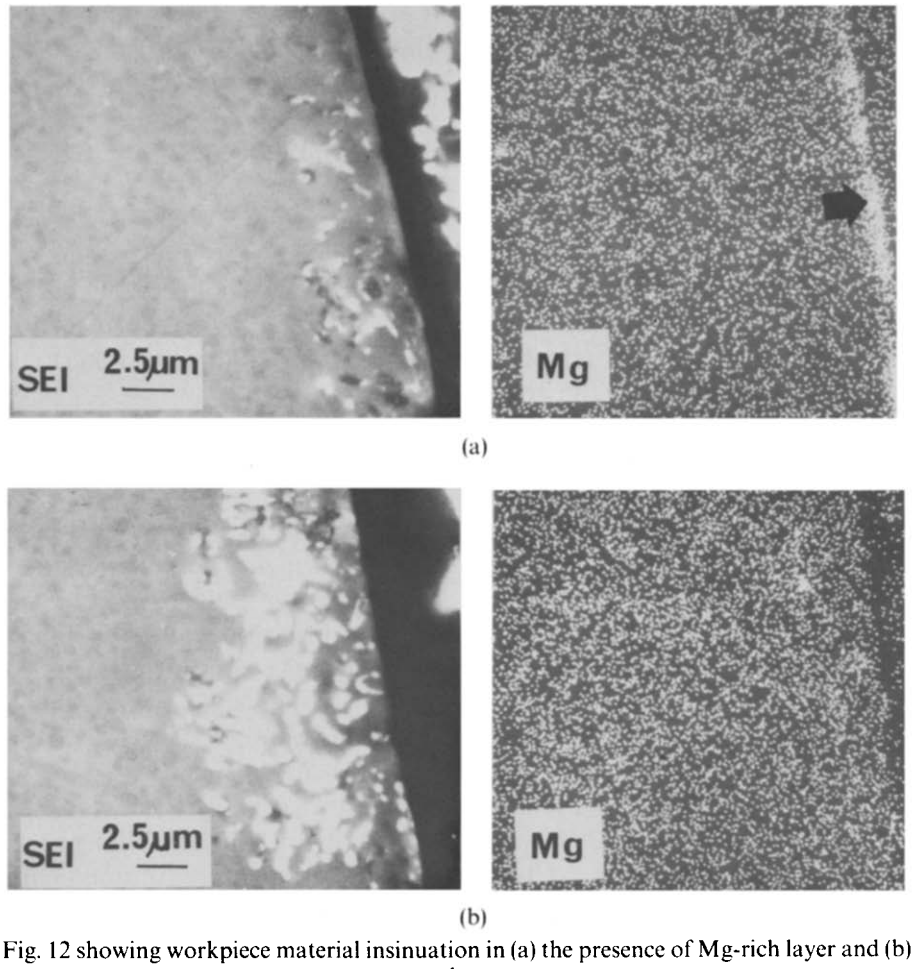

Fig. 15. Detail of Fig. 12 showing workpiece material insinuation in (a) the presence of Mg-rich layer and (b) the absence of Mg-rich layer.

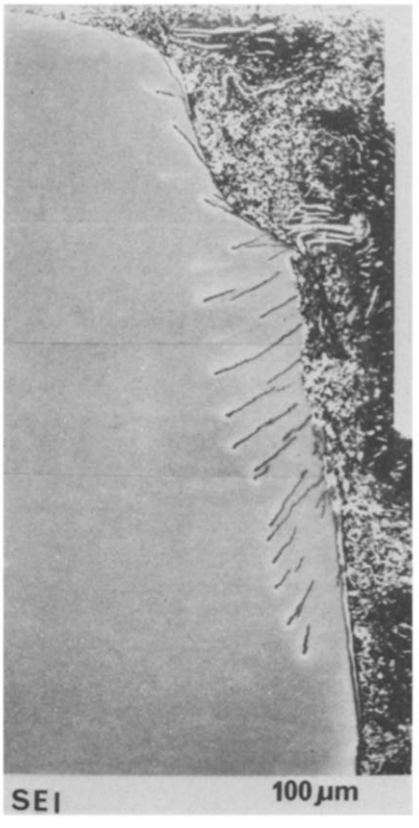

Fig. 16. Section of CC 680 after 1·8 min at 450 m/min (secondary electron scanning electron micrograph).

are not normally observed. The occurrence of cracks in this case is a result of the tool being used at too high a cutting speed.

Figure 17 shows a transverse section and the corresponding elemental distribution. Workpiece material has penetrated very long distances down the thermal cracks and into the tool material. In the surface region it is observed that Ni, Fe and Cr mainly diffuse along the grain boundaries into the tool. Ti, Nb and Al form a coating on the tool surface. Al and O react to form an aluminium oxide coating. A line scan analysis (Fig. 18) from the same area shows that a (Ti,Nb)-nitride coating was formed immediately underneath the aluminium oxide coating. Cr and Ni are found between the silicon nitride grains.

Figure 19 from the lower part of the flank shows that the aluminium oxide coating has been plastically deformed during the metal cutting process.

3.5 DOC and trailing edge notch wear

Notch wear at the depth of cut point had already developed after a few seconds in cut (Fig. 20(a)) as shown for CC 670. Wear is observed both on the rake and flank face. After 1 min in cut the DOC notch wear was well developed (Fig. 20(b)). At high magnification the DOC notch wear surface reveals evidence for the occurrence of a fracturing process as debonding, bridging and pull-out can be seen (Fig. 21(a)). The same was experienced by CC 680 (Fig. 21(b)) where the fracture, however, looks more smooth and typical of a high-temperature fracture process.[2]

Figure 22 shows the trailing notch wear corresponding to 10 min in cut (cf. Fig. 6(a)). The trailing edge wear is more orientated towards the flank face than depth of cut notch wear.

4 SS 2541

4.1 Cutting conditions

The machining tests were performed as a continuous turning operation of cylindrical bars with an original diameter of 185 mm. All tests were performed dry using a 35 kW Swedturn 12 CNC lathe. The same tool holder was used as for the machining experiments with IN.718. However, the inserts were in style SNGN 120416 for this test.

4.2 Wear pattern

Figure 23 shows the development of flank wear for CC 670 and CC 620 at different cutting speeds. The flank wear of CC 670 develops rapidly with increased cutting speed.

Figure 24 also shows that significant cratering occurs simultaneously.

4.3 Electron-probe microanalysis of adhering layers and tool workpiece material interaction

Figure 25 shows a section through the flank wear land and it can be seen that silicon carbide whiskers have dissolved into the adhering layers.

5 Discussion

5.1 Inconel 718

Tool life for the sialon material CC 680 was mainly dependent on flank wear, whereas for CC 670 the tool life criterion was DOC notch wear for most of the cutting conditions studied. Both cutting materials showed flank wear and edge line chipping when machining IN 718. From the transverse sections it was shown that wear was mainly concentrated in the area close to the cutting edge. Normally, when machining workpiece materials which form a continuous chip, e.g. steel, the maximum temperature is reached on the rake face some way back from the cutting edge. In IN 718 highly segmented chips are formed and the tool/chip

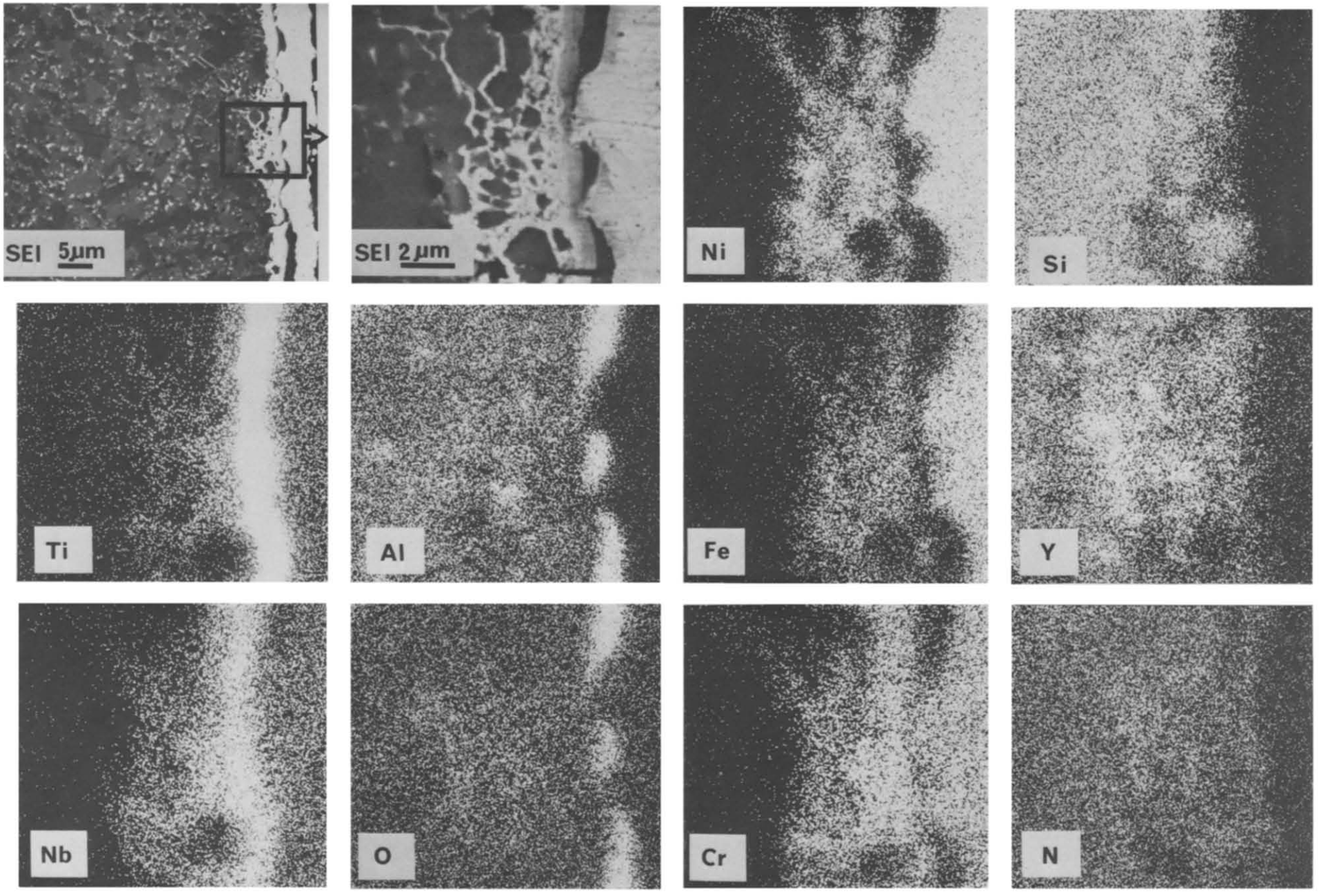

Fig. 17. Details of Fig. 16 and corresponding element distribution.

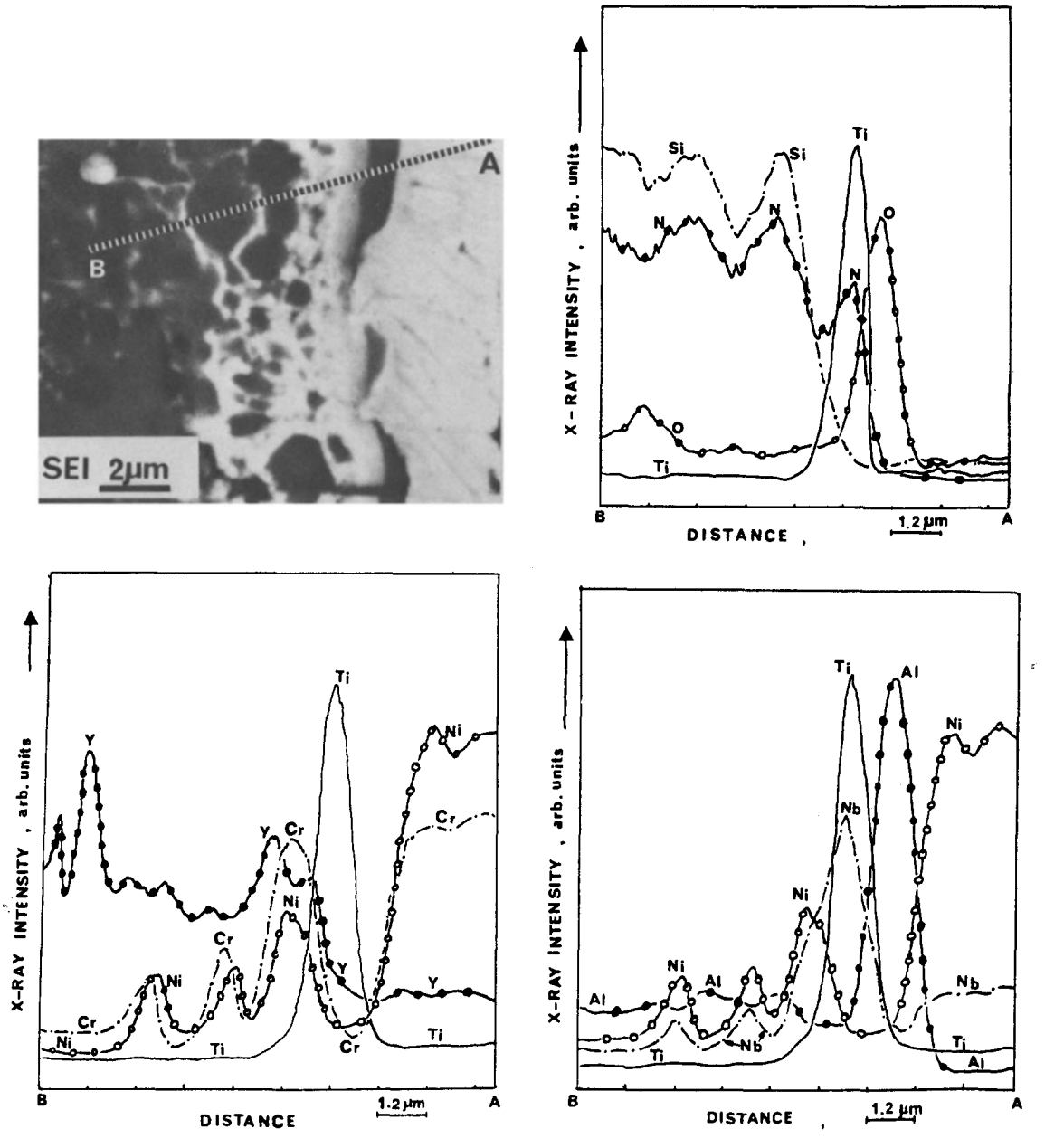

Fig. 18. Distribution of elements along the line A–B on the flank face.

contact length is much smaller, leading to the maximum temperature being situated much closer to the cutting edge. The wear pattern indicates that under these cutting conditions the maximum temperature was situated on the rake face close to the cutting edge.

5.2 Wear mechanisms

5.2.1 Flank wear

5.2.1.1 CC 680. Several mechanisms could be observed to be in operation. Ni, Fe, Cr and Nb penetrate along the grain boundaries and at the same time the oxygen content of the grain boundary phase was reduced (Figs 17 and 18). The alloy formed probably had a low melting point and therefore could easily penetrate along the long paths offered by the thermal cracks (Fig. 17).

A (Ti,Nb)-nitride coating was formed next to the tool material with an alumina coating lying outside it in between the nitride coating and the adhering workpiece material. As shown in Fig. 19 these coatings could give some protection against further penetration of the workpiece material into the tool material. Edge line chipping was most likely a result of an attrition wear process where individual grains or agglomerates were removed from the tool surface due to the strong bonding formed as a result of chemical reaction between the tool and workpiece material. On the lower parts of the flanks where the lower shearing stresses do not remove the coatings

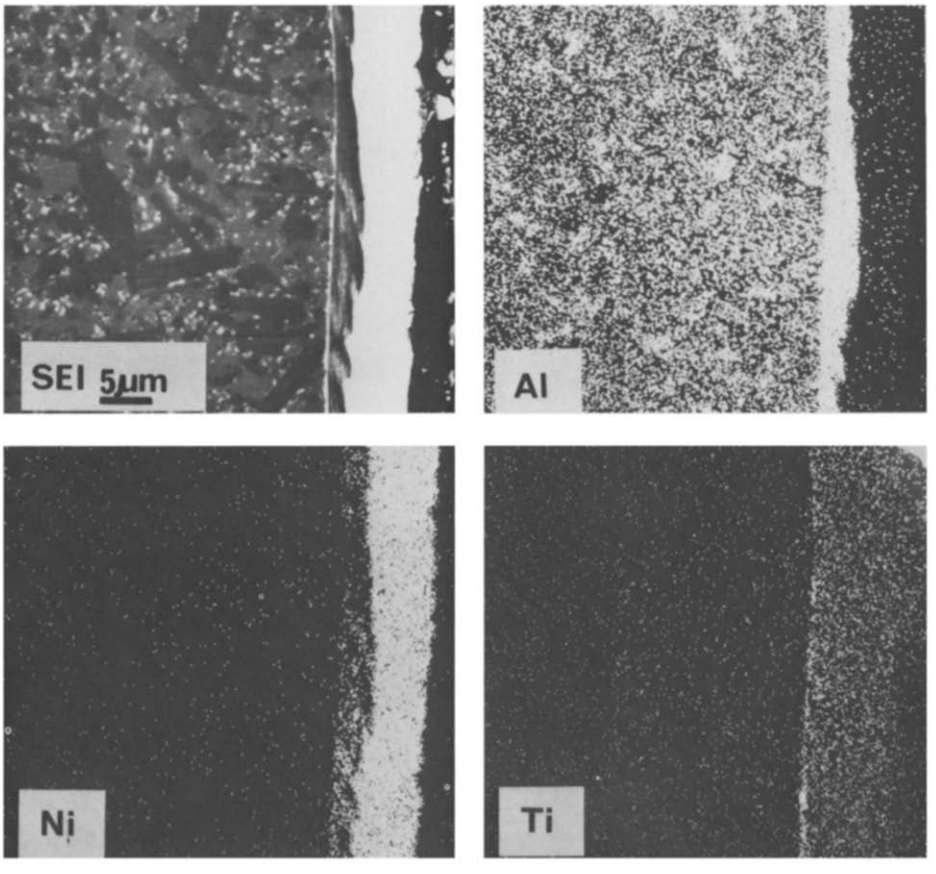

Fig. 19. Detail of Fig. 16 and corresponding element distribution.

during the cutting process the wear was considerably less.

The formation of nitrides during the cutting process was probably a result of a direct reaction between the sialon grains with Ti and Nb. Sialon grains which have been rather heavily attacked can be observed in Fig. 10(c). Aluminium in the workpiece material reacted with oxygen to form alumina. This oxygen emanates at least partly from the tool material which is shown in the line scan analysis in Fig. 18, showing a lower oxygen content in the tool material next to the coatings formed. Another possible explanation could be that atmospheric oxygen reacts with Al on the tool surface. However, this is less likely to occur, since the flank was covered with adhering workpiece material. The formation of nitrides has also been observed when machining another heat-resistant alloy, Incoloy 901.[3]

5.2.1.2 CC 670. The flank wear mechanism for CC 670 seems to be a preferential attack of the silicon carbide whiskers which was accentuated

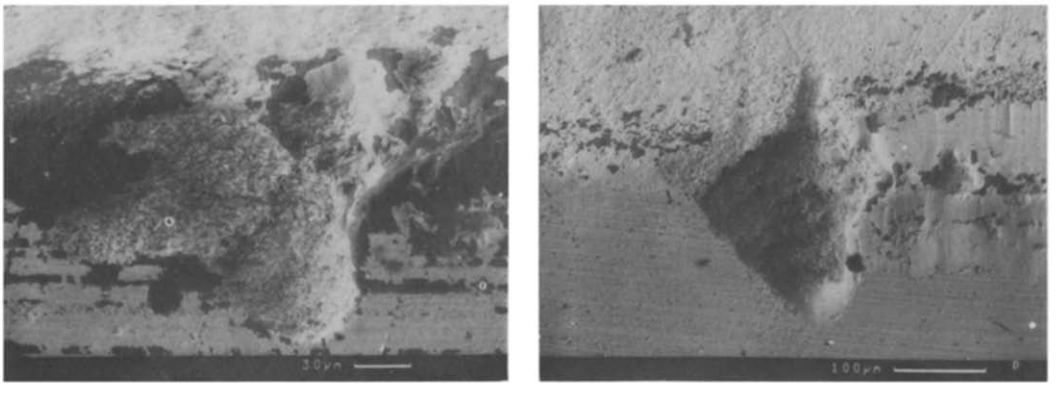

(a) (b)

Fig. 20. DOC notch wear of CC 670 at 150 m/min after (a) 6 s and (b) 60 s.

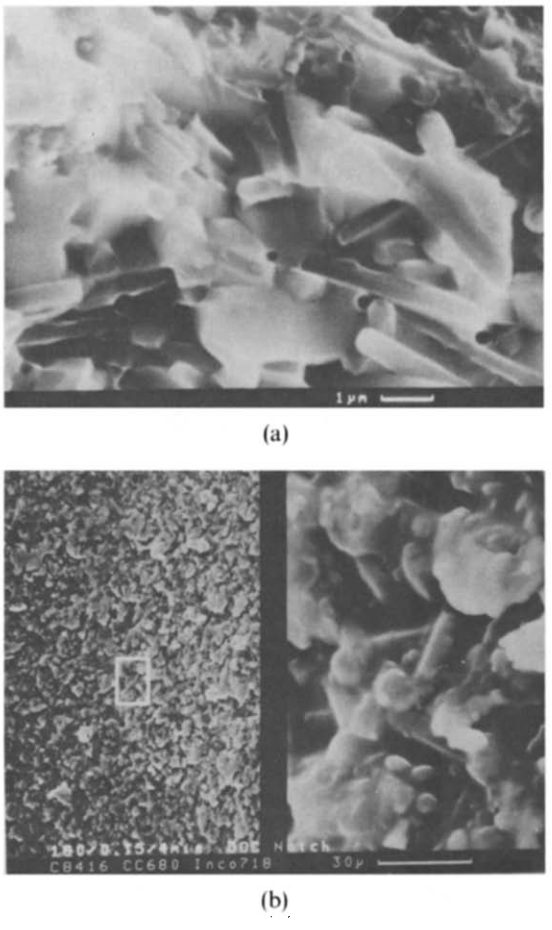

Fig. 21. Detail of DOC notch wear for (a) CC 670 and (b) CC 680.

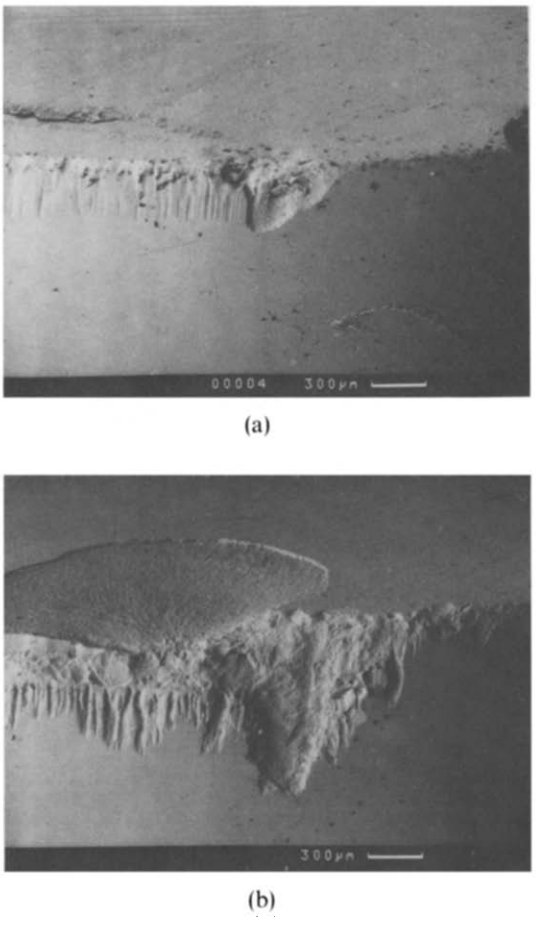

Fig. 22. Trailing edge notch wear after 10 min at 150 m/min at 0·25 mm/rev for (a) CC 670 and (b) CC 680.

upon increasing cutting speed. At the lowest cutting speed some areas were observed where indications of attrition wear process were found (Fig. 7(c)). However, most of the worn flank surface appeared rather smooth, due to the formation of a Mg-rich layer. MgO is used as a deoxidant for Inconel 718[4] and Mg-rich inclusions were also found in this workpiece material (Fig. 26). The magnesium content was determined to be 30 ppm by chemical analysis in the workpiece material used. MgO most probably reacted with alumina to form magnesium aluminate, a compound more deformable than alumina itself,[5] which explains why the worn surface had such a smooth appearance. Figure 14 shows that silicon carbide whiskers are dissolved in the workpiece material and replaced by Ni, Fe and Cr. Ti, Nb, and also to some extent Cr, do not penetrate very great distances into the tool, but form carbides at the tool surface. As these carbides are more stable with regard to dissolution they may offer some protection against further attack by workpiece material along the whiskers.

When the whiskers are replaced by workpiece material and titanium carbide the alumina matrix is undermined and, as shown in Fig. 13, it is likely that single grains and agglomerates of alumina are lost by an attrition-type wear mechanism. In addition the difference in thermal expansion coefficient between the alumina matrix and the metallic workpiece material may cause cracking during cooling at disengagement.

CC 670 was much more resistant towards chemical reactions with the workpiece material. At the lowest cutting speed there was almost no difference

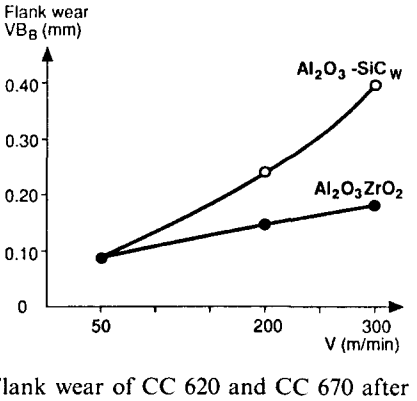

Fig. 23. Flank wear of CC 620 and CC 670 after machining SS 2541 for 5 min at 0·2 mm/rev and 0·5 mm DOC.

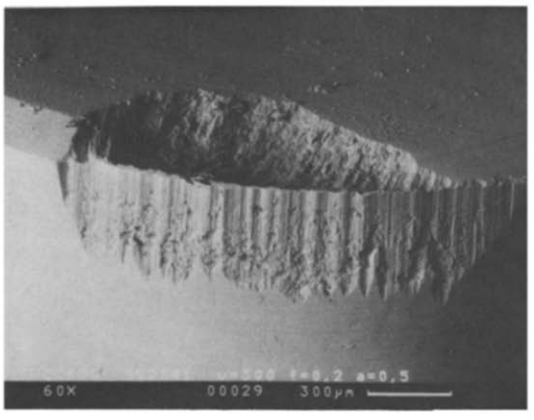

(a)

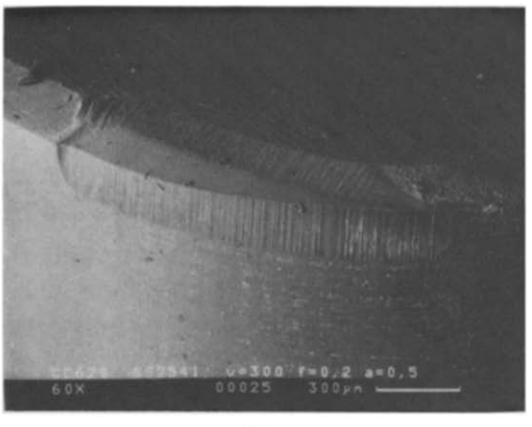

(b)

Fig. 24. Flank and crater wear after machining SS 2541 for 5 min at 300 m/min, 0·2 mm/rev and 0·5 mm DOC for (a) CC 670 and (b) CC 620.

between the two grades, but at 450 m/min CC 680 showed an inferior resistance. This is mainly attributed to the high percentage of the chemically very stable compound alumina in CC 670.

5.2.2 Depth-of-cut notch wear

5.2.2.1 CC 680. At high magnification the worn areas reveal a fracture surface typical for high-temperature fracture of CC 680.[2] As shown in Fig. 27 the chips are highly segmented and the edges of the chips have a typically ragged appearance. This favours an interrupted seizure and breakage process which will lead to pull-out of tool material.[6,7] For good resistance against this type of wear mechanism both good cohesion and toughness are required of the matrix as well as a low reactivity against the workpiece material.

The DOC notch wear process is not a continuous wear process, and as shown in Fig. 5(a) a very large scatter in the wear figures is obtained, due to the statistical nature of this wear process in contrast to flank wear (Fig. 4), which is much more predictable.

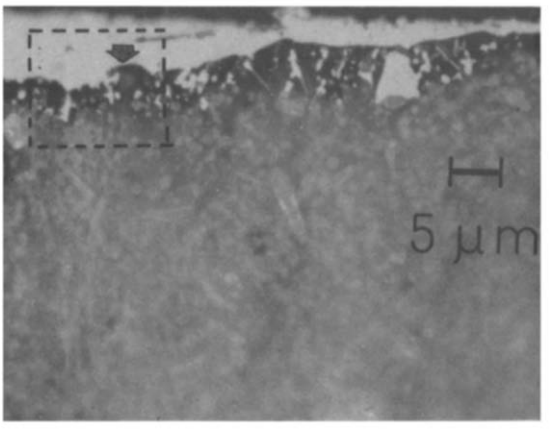

Fig. 25. Section of flank wear of CC 670 after machining SS 2541 for 2 min at 300 m/min. Flank wear surface on top.

5.2.2.2 CC 670. The DOC notch wear developed after very short machining times both on the rake and flank faces. As with CC 680 high magnification revealed a fracture surface, indicating that the same mechanisms were operating for CC 670. Both grades showed about the same resistance to this type of wear mechanism.

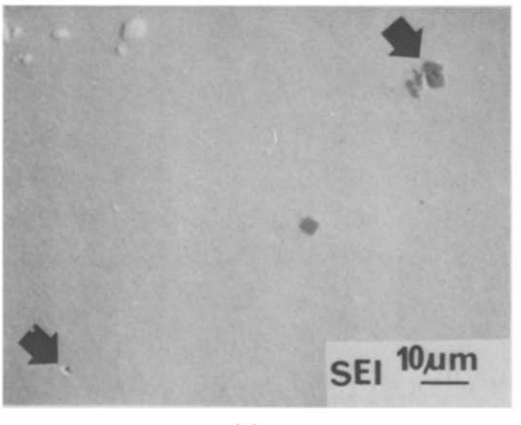

(a)

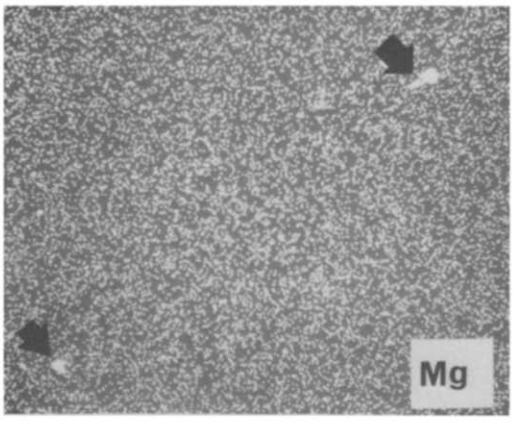

(b)

Fig. 26. Polished section of Inconel 718 and corresponding element distribution of Mg.

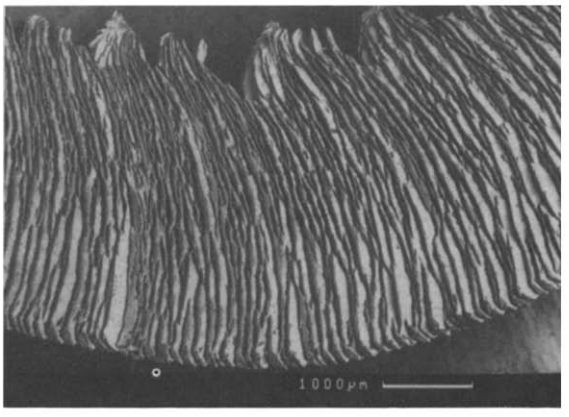

(a)

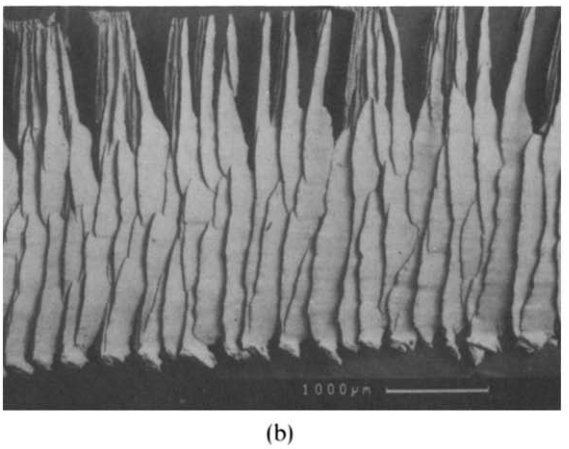

(b)

Fig. 27. Chips after machining Inconel 718 with CC 680 at (a) 150 and (b) 450 m/min.

5.2.3 Trailing edge notch wear

In contrast to the DOC notch wear there is a large difference between the two tool materials with respect to the resistance to this type of wear mechanism. As shown in Fig. 22, the trailing edge notch wear was more orientated towards the flank than the DOC notch wear. At 150 m/min and 0·15 mm/rev there was no difference between the two grades with respect to flank wear resistance, but at 150 m/min and 0·25 mm/rev, used for the surface finishing experiments, flank wear for CC 680 is larger, showing that chemical wear plays a more important role for these cutting data. As the temperature increases with increasing cutting speed or feed and the difference in DOC notch wear between the two grades was insensitive to increases in speed, this indicates that chemical wear plays a more important role for the trailing edge notch wear than for the DOC notch wear.

5.3 Steel SS 2541

In steel the use of silicon carbide whisker reinforced materials is restricted to very low cutting speeds as otherwise there is a rapid dissolution of the whiskers in the workpiece material. The dissolution of silicon carbide in steel is mainly governed by the solubility product.[8] Table 3 shows that the solubility of silicon carbide in iron is several orders of magnitude larger than TiC, for example.

Table 3. Solubilities of tool material constituents in alpha-Fe at 1600 K (1323°C)[8]

Tool constituent	*Solubility (mol %)*
ZrO_2	$3{\cdot}6 \times 10^{-8}$
Al_2O_3	$5{\cdot}6 \times 10^{-7}$
TiN	$1{\cdot}0 \times 10^{-3}$
TiC	$1{\cdot}9 \times 10^{-3}$
SiC	$6{\cdot}4 \times 10^{-1}$

5.4 Comparison between steel and nickel-based alloys

Tool temperature measurements[9] made when machining steel AISI 4340 (similar to SS 2541) and IN 718 (see Fig. 28) indicate a tool temperature which is approximately 200 degrees centigrade higher for IN 718 under identical cutting conditions. As solubility increases with increasing temperature then solution/diffusion wear would be expected to be more severe when machining the heat-resistant alloy.

Another important parameter is the solubility in the workpiece material. Solubility data for SiC in Ni could not be found in the literature and therefore the solubility was calculated theoreticaly. The calculation was made using the POLY program and data available in the THERMO-CALC databases at the Royal Institute of Technology in Stockholm. Information on the binary systems (Fe–C, Fe–Si, Ni–Si and Ni–C) and on the interaction between Si and C in the FCC solid solutions (in case of Ni an estimate) were combined to calculate the iron- and nickel-rich regions of the ternary systems at 1100°C. The results are shown in Fig. 29 and it is shown that the solubility of SiC in Fe and Ni is of the same order of magnitude.

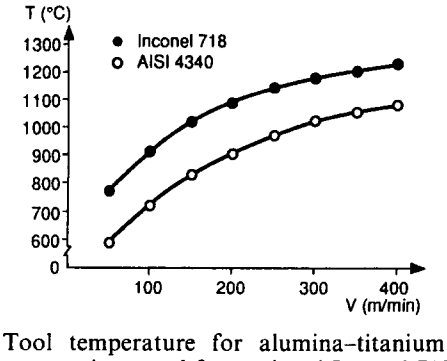

Fig. 28. Tool temperature for alumina–titanium carbide versus cutting speed for steel and Inconel 718.

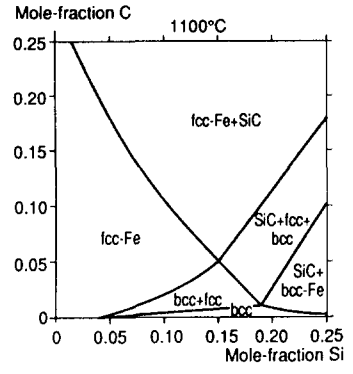

(a)

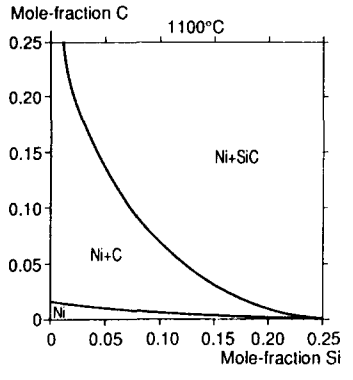

(b)

Fig. 29. Calculated phase diagrams for (a) Fe–Si–C and (b) Ni–Si–C.

If only solution/diffusion wear was operating it would thus be expected that under similar cutting conditions CC 670 would show greater wear when machining the Ni-based alloy. The main reason for the rather unexpected good wear resistance in IN 718 is therefore the formation of magnesium aluminate which creates a diffusion barrier between the whiskers and the workpiece material. The formation of more stable carbides might also to some extent prevent workpiece material from penetrating along the whiskers.

6 Conclusions

The following conclusions are based on turning tests carried out on the heat-resistant workpiece material, Inconel 718, at cutting speeds from 150 to 450 m/min and steel workpiece material SS 2541 at cutting speeds from 50 to 300 m/min.

(1) Flank face wear of sialon and silicon carbide whisker-reinforced alumina was mainly determined by chemical reaction with and dissolution in the workpiece material. The better flank wear resistance of the whisker-reinforced alumina is explained by its better chemical stability.

(2) The DOC notch wear resistance was equal for sialon and the silicon whisker-reinforced alumina. The wear mechanism is mainly mechanical in nature, although chemical reactions may increase the tendency to seizures.

(3) The trailing edge notch wear resistance was better for silicon carbide whisker-reinforced alumina than for sialon. This is probably explained by a higher degree of chemical interaction than at the DOC point.

(4) Both sialon and silicon carbide whisker-reinforced alumina exhibited chipping along the edge line. This was probably caused by an attrition-type wear mechanism.

(5) The unexpected good wear resistance of silicon carbide whisker-reinforced alumina when machining Inconel 718 compared to its use in machining steel SS 2541 is explained by the formation of protective coatings of magnesia compounds and also by the formation of more stable carbides in the surface region.

Acknowledgements

The authors thank AB Sandvik Coromant for permission to publish this paper. Thanks are also due to Dr B. Uhrenius, AB Sandvik Coromant for performing the calculations for the phase diagrams and D. Benton, AB Sandvik Coromant for linguistic scrutiny of the manuscript.

References

1. Brandt, G., Flank and crater wear mechanisms of alumina based cutting tools when machining steel. *Wear*, **112** (1986) 39–56.
2. Brandt, G., Johannesson, B. & Warren, R., Fracture behaviour of selected mixed-ceramic tool materials up to 1200°C. Materials Science and Engineering, Paper presented at the *3rd Int. Conf. on the Science of Hard Materials, Nassau, The Bahamas, November 9–13, 1987*, **A105/106** (1988) 193–200.
3. Bhattacharyya, S. K., Jaward, A., Lewis, M. H. & Wallbank, J., Wear mechanisms of sialon ceramic tools. *Metals Technology*, **10** (1983) 482–9.
4. Alexander, J., Optimizing deoxidation and desulphurization during vacuum induction melting of alloy 718. *Materials Science and Technology*, **1** (1985) 167–70.
5. Brandt, G. & Mikus, M., An electron microprobe and cathodoluminescence study of chemical reactions between tool and workpiece when turning steel with alumina based ceramics. *Wear*, **115** (1987) 243–63.

6. Trent, E. M., *Metal Cutting*. Butterworths, London, 1977.
7. Lee, M., Horne, J. G. & Tabor, D., The mechanism of notch formation at the depth of cut line of ceramic tools machining nickel-base super alloys. In *Proceedings of the Second International Conference on the Wear of Materials*, ASME, New York, 1979, pp. 460–9.
8. Kramer, B. M. & Suh, M. P., Tool wear by solution: A quantitative understanding. *J. Eng. Ind.*, **102** (1980) 303–9.
9. Huet, J. F. & Kramer, B. M., The wear of ceramic cutting tools, In *Proceedings of the 10th North American Metalworking Research Conference*, ed. R. S. Hahn. ASME Dearborn, MI, 1983, pp. 297–304.